

Monitoring the nitrogen nutrition status of rice plants using spectral and image technologies

YE Chun^{1,2}, LIU Jizhong^{1*}, LIU Ying^{1*}, LI Yanda², CAO Zhongsheng², HUANG Huang³

4 1. School of Mechanical and Electrical Engineering, Nanchang University, Nanchang 330031,

5 China;

6 2. Institute of Agricultural Engineering/Jiangxi Province Engineering Research Center of

7 Intelligent Agricultural Machinery Equipment/Jiangxi Province Engineering Research Center of

8 Information Technology in Agriculture, Jiangxi Academy of Agricultural Sciences, Nanchang

9 330200, China;

10 3. Engineering College of Huazhong Agricultural University, Wuhan, 430070, China.

11

12 *Corresponding author: LIU Jizhong

13 Tel: 0791-83969629/13970070635

14 Email: jizhongl@163.com

15

16

17 **Abstract**

18 **Background:** We aimed to investigate methods to estimate the nitrogen (N) nutrition status of rice
19 plants using data obtained using a digital camera and a spectroradiometer. The overall aim was to
20 compare the advantages and potential of image technology and spectral technology to monitor rice
21 N indexes accurately, inexpensively, and in real time to optimize fertilization strategies. Realizing
22 the technical selection of definite spectrum or image diagnosis aiming at different rice nitrogen
23 nutrition indexes. We conducted field trials of rice plants grown with different levels of N fertilizer
24 in 2018 to 2019. Spectral information and images of the rice canopy were obtained, various image
25 and spectral characteristic parameters were selected to construct models to estimate rice N status.

26 **Results:** The determination coefficients of the models constructed using the ratio vegetation index
27 ($RVI_{[800,550]}$) and cover canopy (CC) as dependent variables were most significant. Among the
28 models using spectral parameters, those constructed using $RVI_{[800,550]}$ to estimate rice N indexes had
29 the obviously coefficient of determination (R^2) values, which were 0.69, 0.58, and 0.65 for the
30 models to estimate leaf area index(LAI), aboveground biomass(AGB), and plant N
31 accumulation(PNA). As for image parameter, those using CC to predict rice N indexes showed the
32 highest R^2 values (0.76, 0.65, and 0.71 for the models to estimate LAI, AGB, and PNA, respectively)
33 ($P < 0.01$). The model using the spectral parameter $RVI_{[800,550]}$ had a good fit and stability in
34 estimating plant nitrogen accumulation ($R^2 = 0.65$, root mean square error (RMSE) = $1.35 \text{ g} \cdot \text{m}^{-2}$,
35 relative RMSE (RRMSE) = 14.05%), and the model using the image parameter CC had a good fit
36 in predicting leaf area index ($R^2 = 0.76$, RMSE = 0.28, RRMSE = 7.26%) and aboveground biomass
37 ($R^2 = 0.65$, RMSE = $22.03 \text{ g} \cdot \text{m}^{-2}$, RRMSE = 7.52%). Different detection technology should be
38 adopted for different rice varieties and rice N nutrition indexes.

39 **Conclusions:** Spectral and image parameters can be used as technical parameters to estimate rice N
40 status. The spectral parameter $RVI_{[800,550]}$ can be used to accurately estimate plant nitrogen
41 accumulation, and the image parameter CC can be used to accurately estimate leaf area index and
42 aboveground biomass.

43 **Key words:** image; canopy coverage; spectral index; rice; nitrogen nutrition

44 **Background**

45 Rice (*Oryza sativa* L.) is one of the most important food crops both in China and around the world.
46 It plays an important role in food security, and provides social and socioeconomic stability. Nitrogen
47 (N) is one of the most important nutrients for the growth and development of rice plants. In China,
48 the amount of N fertilizer applied to rice crops accounts for 37% of the N fertilizer used globally.
49 However, the average utilization rate of N fertilizer is only 35% [1]. Increasing N applications can
50 increase rice yield, but excessive N application causes a series of environmental problems, such as
51 greenhouse gas emissions, soil acidification, and water pollution [2, 3]. In addition to nitrogen
52 management, rice breeding also plays an important role in the process of increasing rice yield. GAO
53 et al. [4] showed that hybrid rice had heterosis compared with conventional rice, the yield increase
54 advantage mainly depends on the dry matter production advantage of aboveground plants. Therefore,
55 the scientific and rational application of N fertilizer and study the difference of nitrogen nutrition
56 between hybrid rice and conventional rice are of great significance for high-yielding rice.

57 Accurate N management is an essential part of the rice production management system.
58 Accurate determination of the N nutrition status of rice is essential for accurate N management [5].
59 Leaf area index (LAI), aboveground biomass (AGB), and plant nitrogen accumulation (PNA) are
60 important indicators that are used to characterize rice growth and N status [6]. They are usually

61 determined by chemical analyses, which provide accurate results [7]. However, the disadvantages
62 of chemical analyses are their high cost, lengthy and complex operation, and the need for expensive
63 and potentially harmful chemical reagents. For these reasons, chemical analyses are insufficient to
64 meet the needs of real-time monitoring of N nutrition in large-scale crops [8]. One alternative is to
65 use near-ground hyperspectral equipment to monitor the N status of crops in a large area. Willkomm
66 et al. used low-cost unmanned aerial vehicles to generate a high-resolution crop surface model
67 (CSM) for rice. On the basis of comparisons of agronomic parameters (fresh and dry AGB, LAI,
68 and plant nitrogen concentration) measured using hyperspectral methods and direct methods, it was
69 concluded that the plant height of rice was significantly correlated with fresh AGB and LAI
70 (coefficient of determination, $R^2 > 0.8$) [9]. He et al. accurately estimated N distribution in the vertical
71 leaves of the rice canopy using a knapsack spectrometer, and the hyperspectral model was shown to
72 have good predictability [10]. In addition, some special instruments for plant nutrition diagnosis
73 have been developed, such as the SPAD chlorophyll meter [11] and the GreenSeeker spectrometer
74 [12]. A portable spectrometer is easy to carry and use, but one of its disadvantages is that the
75 diagnostic results are not reliable for crops with excess N absorption [13]. Consequently, this method
76 cannot be used to evaluate crops growing with an excess of N.

77 Digital cameras are a common and inexpensive piece of equipment. They can collect image
78 and spectral information with sufficient quality to use in predictions of crop nutrition status [13, 14]
79 and yield [15] [16], and to monitor pests [17]. Li et al. extracted the dark green color index (DGCI)
80 of image features, and concluded that DGCI was significantly correlated with the SPAD value of
81 rice leaves. Thus, DGCI could be used to estimate the chlorophyll value of rice leaves and indirectly
82 evaluate the growth and nutrition status of rice [18]. Jia et al. used a digital camera and a

83 Greenseeker hand-held sensor to monitor cotton growth and N status[19]. The results revealed an
84 exponential relationship between the image parameter canopy cover (CC) and aboveground total N
85 content. The R^2 value of the model was 0.926, and the root mean square error (RMSE) value was
86 $1.631 \text{ g} \cdot \text{m}^{-2}$. Lee et al. used image red-green-blue (RGB) parameters and CC to monitor rice
87 nutrition status in real time [13, 20]. They established a stepwise multiple linear regression model
88 based on a non-linear relationship between rice color indexes and CC. Using this model, information
89 about the nutrient status of crops could be obtained quickly and non-destructively using image
90 technology [21]. Models to predict leaf area index (LAI), biomass, and plant N accumulation (PNA)
91 have been constructed using various methods. However, less attention has been paid to the
92 advantages and disadvantages of spectral and image techniques in monitoring nitrogen nutrition in
93 rice. Rice yield is affected by many factors, among which the succession of rice varieties and the
94 improvement of fertilization measures play an important role in the formation of rice yield.

95 Hence, the objectives of this study were to: (1) assess the potential of rice canopy image
96 parameters to monitor hybrid rice and conventional rice N status; (2) compare and analyze models
97 based on image and spectral parameters to estimate rice N status; and (3) determine the accuracy,
98 advantages, and disadvantages of the models constructed using different image and spectral
99 parameters. The overall aim of our research was to provide a reference for the fast, inexpensive, and
100 non-destructive monitoring of the N status of rice crops.

101 **Results**

102 **Relationships Between Rice N Nutrition Indexes and Image/Spectral parameters**

103 During the whole growth period of rice, the correlations between image or spectral parameters and
104 N nutrition indexes of the whole growth period of rice were analyzed (Table 1). There were

105 significant differences in the correlation coefficients between image and spectral parameters. The
 106 spectral parameters were all positively correlated with rice N indexes. RVI_[800,550] was most
 107 correlated with PNA, DVI_[800,720] was most correlated with LAI and AGB, and that the correlation
 108 coefficients ranged from 0.419 to 0.645. Different from spectral indexes, canopy coverage (CC),
 109 red normalized value (NRI) and hue (H) were significantly correlated with aboveground biomass,
 110 nitrogen accumulation and LAI of rice ($P < 0.01$), and the correlation coefficients ranged from 0.427
 111 to 0.831. Among them, NRI was negatively correlated with rice N indexes, while Hue and CC were
 112 positively correlated with rice N indexes. The correlation coefficient between NRI and aboveground
 113 biomass, plant nitrogen accumulation and LAI was the highest, with an average of 0.74 ($P < 0.01$).
 114 Although there was a significant correlation between other parameters and N nutrition index of rice,
 115 the correlation coefficient was very low. Therefore, the image parameters CC, NRI, Hue and spectral
 116 index RVI_[800,550] and DVI_[800,720] were selected as sensitive parameters to construct rice N nutrition
 117 monitoring model furthermore.

118 **Table 1**

119 **Correlations between rice N indexes (LAI, biomass, PNA) and image/spectral parameters**

Image parameter				Spectral parameter			PNA
	LAI	AGB	PNA	LAI	AGB		
NRI	-0.685**	-0.828*	-0.698**	RVI _[800, 550]	0.572**	0.064**	0.574**
NGI	-0.071*	-0.311**	-0.316*	RVI _[800, 720]	0.504**	0.248*	0.512**
GDR	0.549	0.758	0.135	DVI _[800, 720]	0.645**	0.462**	0.419**
GMR	-0.109*	-0.493**	-0.088*	NDVI _[800, 680]	0.493**	0.158**	0.438**
Hue	0.707*	0.685*	0.427*	λ_{rep}	0.298**	0.069**	0.275**

CC	0.619**	0.831**	0.595**
----	---------	---------	---------

120 Note: ** correlation significant at the 0.01 level, * correlation significant at the 0.05 level.

121 **Construction of Rice N Nutrition Models Based on Image/Spectral Parameters**

122 1) Models based on spectral parameters

123 Select the data of jointing period to build the model. The spectral parameters ($RVI_{[800,550]}$ and

124 $DVI_{[800,720]}$) calculated in experiment 1 and experiment 2 were used as independent variables to

125 predict N indexes of rice. The relationships between $RVI_{[800,550]}$, $DVI_{[800,720]}$ and N nutrition indexes

126 of rice were all polynomial functions. The R^2 values for models using $RVI_{[800,550]}$ to predict LAI,

127 AGB, and PNA were 0.69, 0.58, and 0.65, respectively ($P < 0.01$). And for $DVI_{[800,720]}$ the coefficient

128 were 0.54, 0.55, and 0.55, respectively ($P < 0.01$)(Fig.2).

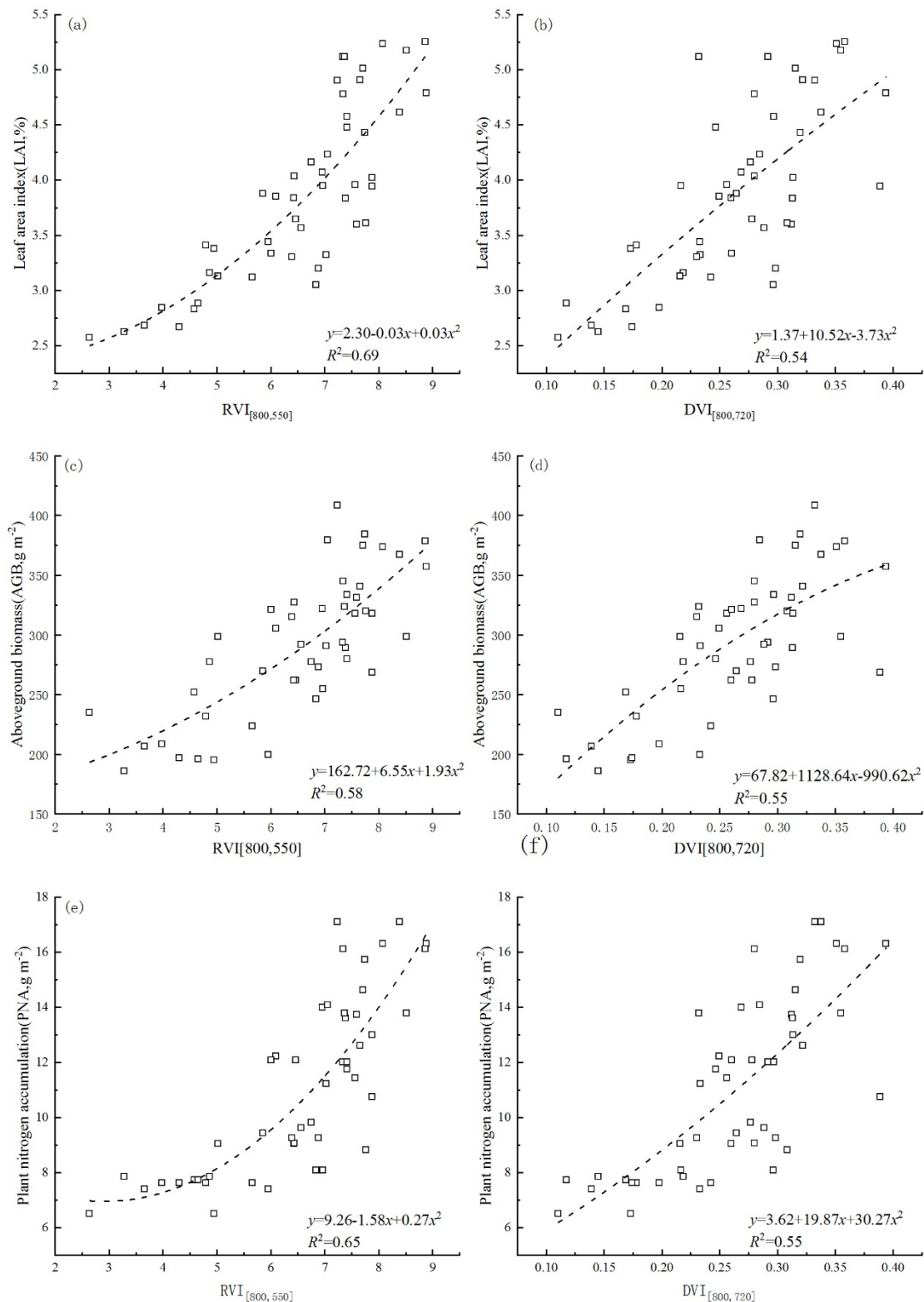
129 Take $DVI_{[800,720]}$ as an example, there were significant differences between conventional rice and

130 hybrid rice in the application of spectral parameters to predict rice nitrogen status. The relationships

131 between $DVI_{[800,720]}$ and the N indexes of rice were all polynomial functions, the accuracy of

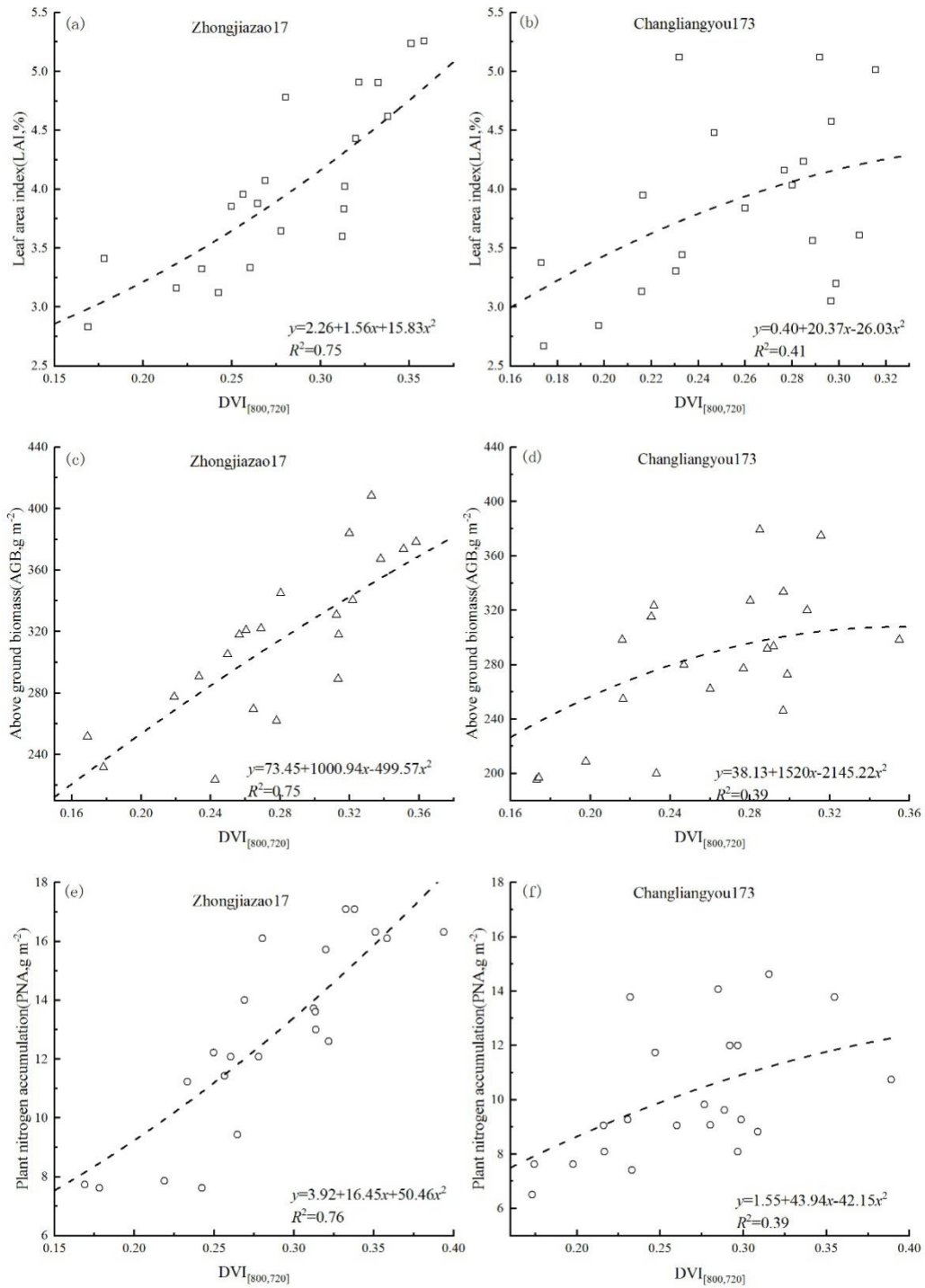
132 monitoring rice N indexes by $DVI_{[800,720]}$ in Zhongjiaozao 17 was higher than that in hybrid rice

133 Changliangyou173(Fig.3).



134

135 **Fig. 2 Relationships between RVI_[800,550], DVI_[800,720] and rice N indexes**



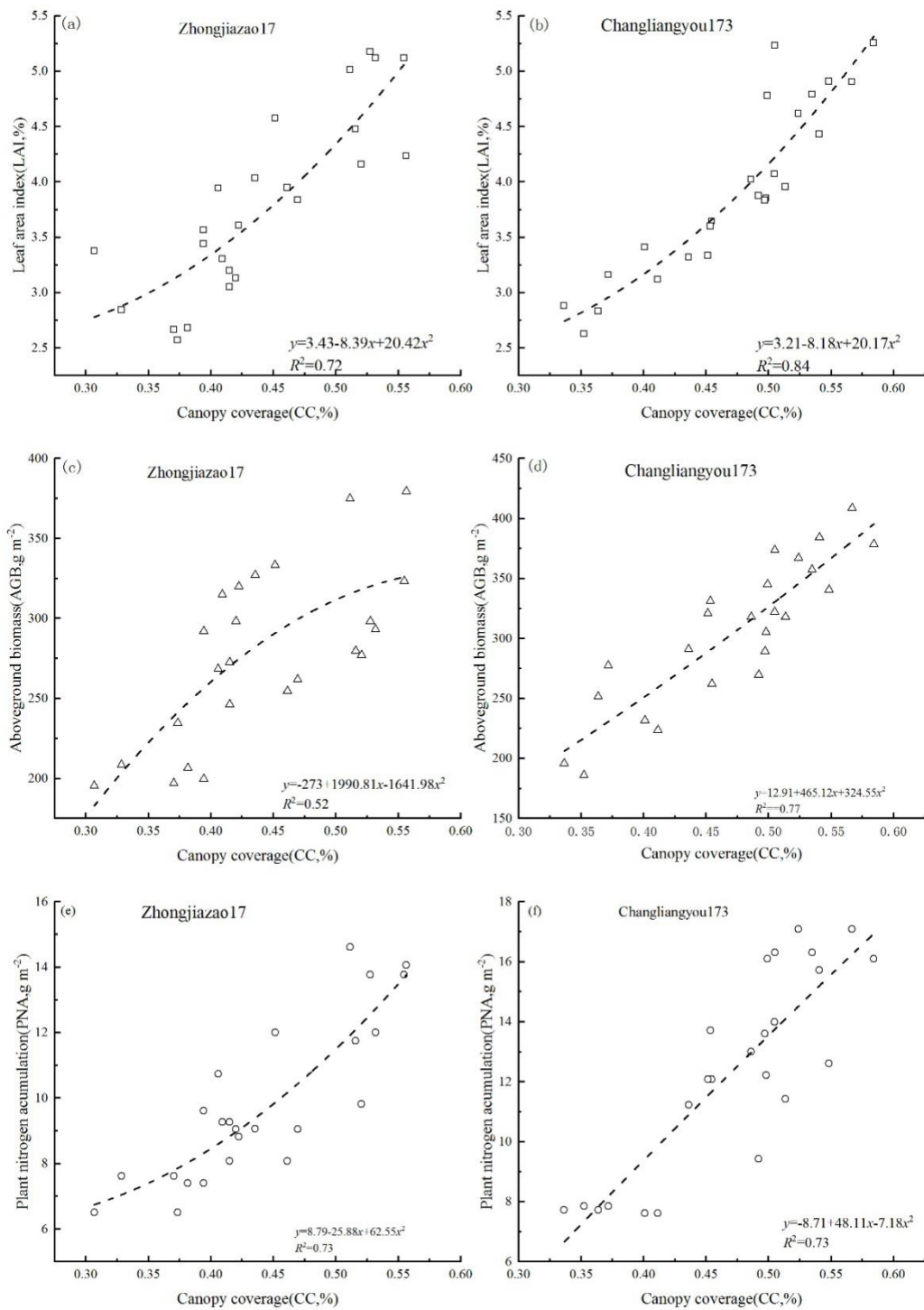
136

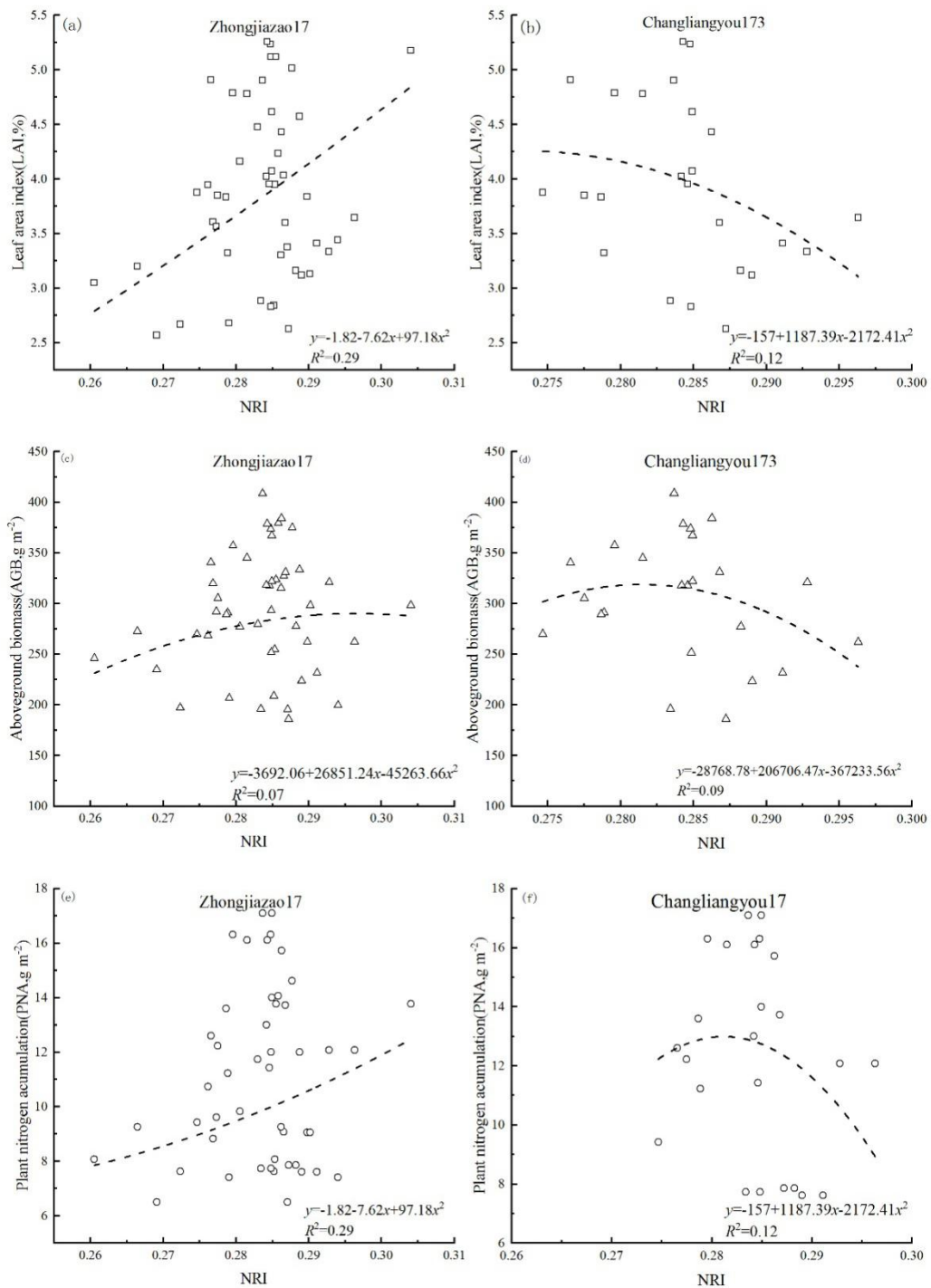
137 **Fig. 3 Relationships between DVI_[800,720] and rice N indexes**

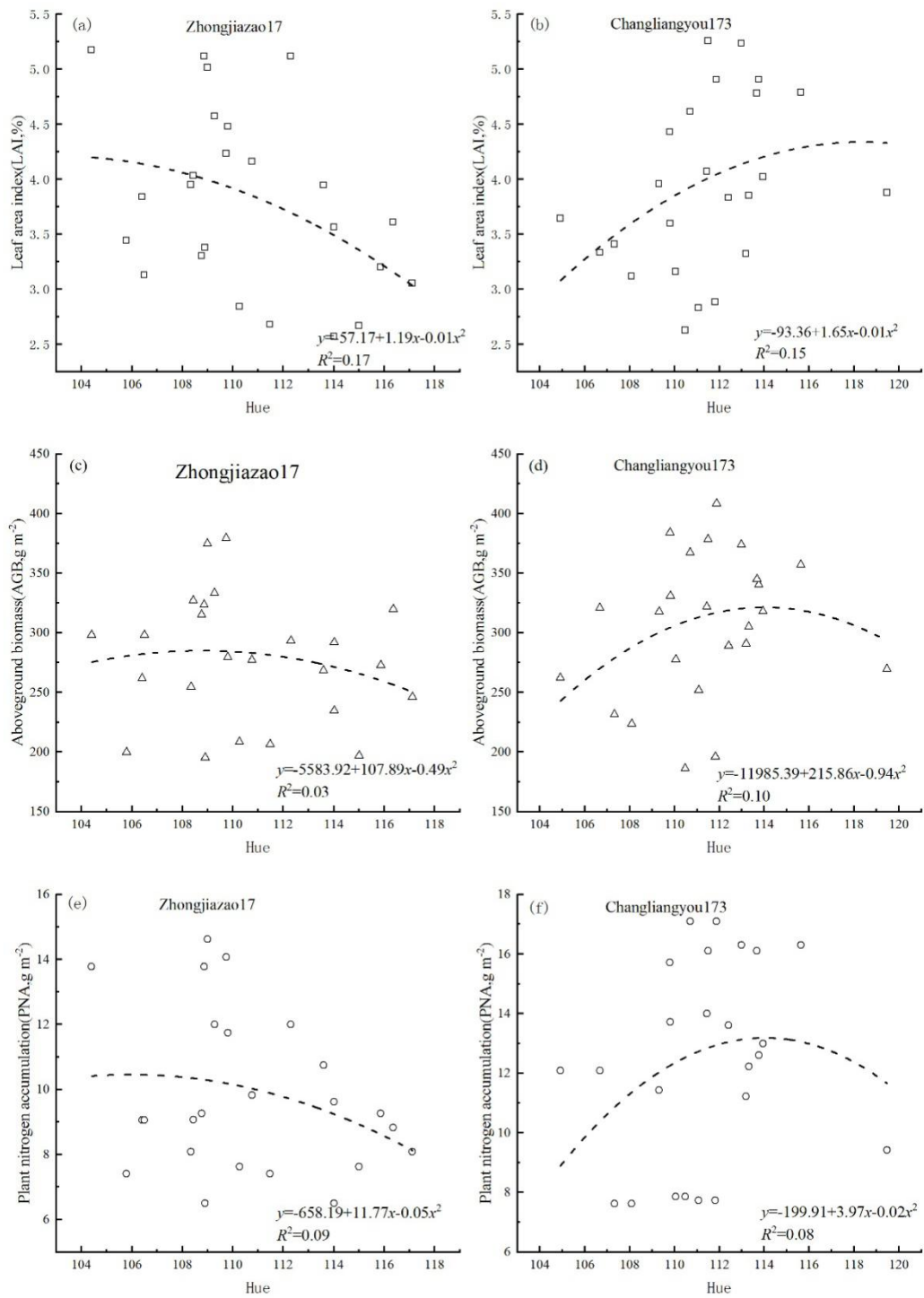
138 2) Models based on image parameters

139 The relationships between CC and N nutrition indexes of rice were all polynomial functions. The

140 R^2 values for models using CC to predict LAI, AGB, and PNA were 0.76, 0.65, and 0.71,
141 respectively ($P < 0.01$). LAI, aboveground biomass and plant nitrogen accumulation of rice
142 increased with the increase of CC, while the correlation coefficients between NRI, Hue and rice N
143 indexes were not significant($R^2 < 0.5$), the average correlation coefficient of NRI model was 0.16,
144 and that of hue was 0.10. As for conventional rice and hybrid rice in the application of CC to predict
145 rice nitrogen status, the average coefficient of models based on CC in hybrid rice Changliangyou173
146 was 0.74, which was higher than that in conventional rice Zhongjiaza017.
147 It can be seen from the above that the models based on RVI_[800,550] and CC had good prediction
148 effect for rice N indexes, and there were significant differences among different gene varieties.







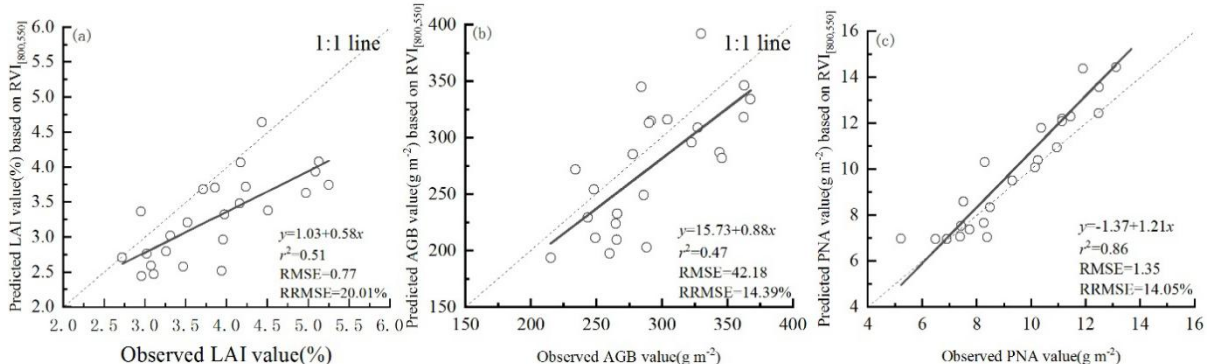
153

154 **Fig. 6 Relationships between Hue and rice N indexes.**

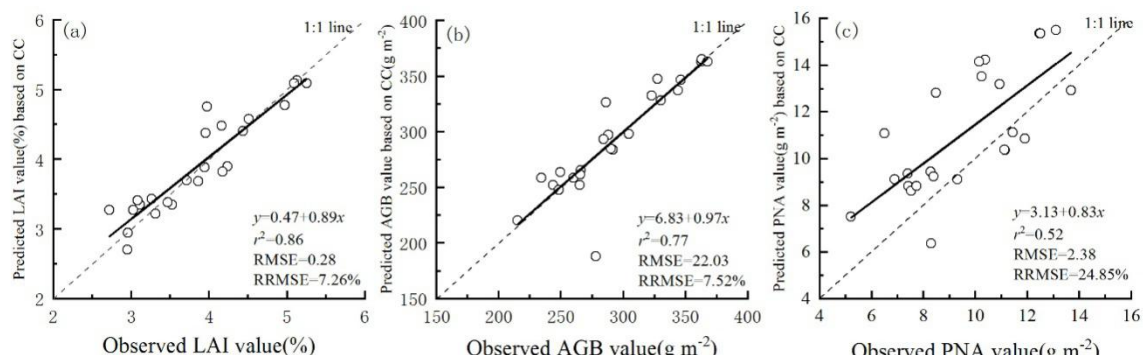
155 3) Regression validation

156 To test the accuracy of the models, those based on the spectral parameter RVI_[800,550] and the image

157 parameter CC were tested and evaluated using data from experiment 3 obtained at the jointing stage
 158 (Fig. 7, Fig.8). The RMSE, RRMSE, and r^2 values were calculated to evaluate the accuracy and
 159 stability of the models. The result showed that the r^2 from $RV_{[800,550]}$ regression equations were
 160 0.51, 0.47 and 0.86 respectively, and that the RMSE values were 0.77, 42.18 and 1.35, respectively
 161 (Fig. 7a, 7b, 7c). As shown in Fig. 8, there was good consistency between the observed value and
 162 the value predicted by the model constructed using the image parameter CC as the independent
 163 variable except for predict PNA (r^2 values of 0.86, 0.77, and 0.52 for LAI, AGB, and PNA,
 164 respectively; $P < 0.05$). The RMSE values from CC regression equations were 0.28, 22.03 and 2.38,
 165 respectively (Fig. 8a, 8b, 8c). Among all the models, the PNA model based on $RV_{[800,550]}$ showed
 166 ideal test result, with a higher r^2 and smaller RMSE , RRMSE values than that from CC regression
 167 equations, while the test result of LAI and AGB equations based on CC showed better result with
 168 higher r^2 and smaller RMSE , RRMSE values than that from $RV_{[800,550]}$ regression equation.



170 **Fig. 7. Relationship between observed values in rice plants and predicted values from models based on**
 171 **$RV_{[800,550]}$.**



174 **Fig. 8 Relationship between observed values in rice plants and predicted values from models based on CC.**

175 **Discussion**

176 **Comparison of Methods to Estimate Rice N Status**

177 In recent years, accurate and non-destructive spectral and image techniques have been developed
178 for the real-time monitoring of crop growth and N nutrition[21, 22]. However, few studies have
179 compared and contrasted models constructed using data obtained using these two techniques.

180 Hyperspectrometry has many advantages, including precise measurements and abundant spectral
181 data [23, 24]. Single bands readily become saturated, it is better to use data from two or more bands
182 as spectral parameters to create models to estimate the biochemical parameters of vegetation [25].

183 In the present study, $RV_{[800,550]}$, a dual-band vegetation index at the jointing stage, was used as an
184 independent variable in models to estimate the N status of rice. The R^2 values of models using
185 $RV_{[800,550]}$ to estimate LAI, AGB, and PNA were 0.69, 0.58, and 0.65, respectively. While the
186 models using $DVI_{[800,720]}$ had poor fitting abilities. Different spectral parameters have different
187 effects in different application environments. Zhao et.al. [26]constructed a regression model of a

188 maize N nutrition index using a dual-band spectral index (R_{710}, R_{512}), and it was proven to be a very
189 good predictor. Sun et al . [27] used hyperspectral technology and BP neural network to establish
190 the estimation model of nitrogen concentration in rice leaves , which was better than the traditional
191 multiple linear regression model. The results showed that the dual-band vegetation index model and
192 BP neural network model were better than the traditional multiple linear regression model, but the
193 cost of hyperspectral technology was high and the operation was complicated.

194 Compared with spectral technology, image technology does not need special equipment to
195 diagnose crop N status. This greatly reduces the cost of detection and provides a reliable basis for

196 precision agriculture. The intensity of R, G, and B colors in the canopy image provides information
197 about most plant organs. The quantification of the intensity values of these visible colors (R and G)
198 can describe plant color [28], which can reflect its nutrient status, especially N content and
199 absorption. Several studies have shown that RGB color space parameters extracted from vegetation
200 canopy images can be used to predict vegetation yield and nutrient status [15, 19, 20]. Among the
201 models constructed with image parameters in this study, those constructed using NRI were unstable,
202 possibly because the parameters of NRI were obtained by extracting RGB values from images.

203 These values can be affected by the time and the weather when the image was acquired. The model
204 constructed using CC had a good fitting effect. The R^2 values of the models using CC to estimate
205 LAI, AGB, and PNA were 0.76, 0.66, and 0.71, respectively, consistent with the conclusion that CC
206 is a reliable parameter to estimate vegetation N content [29]. The CC value is obtained by removing
207 the influence of soil and water in the image. Compared with other image parameters, CC is obtained
208 more easily and is not affected by weather or light intensity.

209 **Advantages and Disadvantages of Models using Spectral and Image Parameters**

210 The results of previous studies indicated that the booting stage is the peak period of rice plant growth,
211 when the LAI is the highest. The booting stage is considered as the best time and cut-off point for
212 estimating rice yield using remote sensing. However, some other studies have found that the early
213 heading stage is the best time to use the spectral index RVI and color indexes to estimate rice LAI
214 [30, 31]. In our study, through the correlation analysis of spectral parameters and image parameters
215 with the nitrogen nutrition index of the whole growth period of rice, the parameters with larger
216 correlation value were selected for modeling. According to the practice of fertilization in the double
217 cropping rice region of southern China, the last fertilizer, panicle fertilizer, must be applied before

booting stage to supply the nutrition needed after booting. Therefore, in order to achieve accurate fertilization before booting, the data of jointing stage were used for modeling. The results of the comparative analysis of the constructed models (Table 2) showed that the stability (RMSE value) of the model using CC to predict PNA was lower than that using $RVI_{[800,550]}$. While to predict LAI and AGB, they were higher than that using $RVI_{[800,550]}$. Among all the constructed models, the model to estimate LAI using CC had a high fitting ability and good stability (higher R^2 value, small RMSE value). The fitting ability of the model to predict AGB using CC was also high (higher R^2 value, small RMSE value). In general, the model using the spectral parameter $RVI_{[800,550]}$ to predict PNA had a good fitting ability and good stability, while the model using the image parameter CC to predict LAI and AGB had a good fitting ability and stability. From the viewpoint of LAI, AGB prediction, CC can be used as alternative technical parameters for estimating, and $RVI_{[800,550]}$ can be used as alternative technical parameters for estimating PNA.

Table 2 Comparison of model test results

Dependent variable	Independent variable	Estimation model	R^2	RMSE	RRMSE(%)	r^2
$RVI_{[800,550]}$	LAI	$y = 2.31 - 0.03x + 0.03x^2$	0.69	0.77	20.01	0.51
	AGB	$y = 162.72 + 6.55x + 1.93x^2$	0.58	42.18	14.37	0.47
	PNA	$y = 9.26 - 1.58x + 0.27x^2$	0.65	1.35	14.05	0.86
CC	LAI	$y = 3.34 - 8.08x + 19.75x^2$	0.76	0.28	7.26	0.86
	AGB	$y = -88.71 + 1022.24x - 403.05x^2$	0.65	22.03	7.52	0.77
	PNA	$y = 3.11 - 4.40x + 46.88x^2$	0.71	2.38	24.85	0.52

In addition, different rice varieties also had influence on model construction. The difference in

232 nitrogen nutrition diagnosis between hybrid rice and conventional rice may also be related to
233 nitrogen use efficiency. Previous studies have shown that the nitrogen accumulation in hybrid rice
234 is significantly higher than that in conventional rice as the nitrogen supply level increases[4]. Peng
235 et al. [32]indicated that the application ratio of panicle fertilizer should be increased to promote
236 nutrient absorption and accumulation in the middle and late growth stage of hybrid rice. There was
237 a significant correlation between vegetation reflection and nitrogen accumulation, which could be
238 analyzed using multi-term linear regression method[33], consistent with this study. Moreover, the
239 correlation between crop population reflection spectrum and nitrogen accumulation was better than
240 that between digital image and nitrogen accumulation. The two-band combination has advantages
241 in the inversion of nitrogen accumulation.

242 An effective strategy to optimize N use for rice should be suitable for the methods used by farmers,
243 while taking account of factors such as cultivars that affect the N requirements of rice and the
244 efficiency of its use. There are still many uncertain factors in remote sensing of crop N status. In
245 this study, we did not consider the effects of several imaging factors (shooting angle, storage format,
246 shooting time, and camera resolution). To obtain a reliable and universal model, it is necessary to
247 further standardize imaging factors, test varieties, growth period, and test points, and to integrate
248 soil and climate data. This will improve the accuracy of models so that they can be used to quickly
249 diagnose the nutrient status of field crops and establish a tailored fertilization system.

250 **Conclusion**

251 In this study, we constructed models to estimate rice N indexes with the image parameter and
252 the spectral parameter. We analyzed the accuracy and stability of the models to predict LAI, AGB,
253 and PNA. The results showed that the R^2 values of the models constructed with the image parameter

254 CC and the spectral parameter $RVI_{[800,720]}$ were very significant. Compared with other models, the
255 polynomial model constructed using CC to predict LAI ,AGB and the model constructed using
256 $RVI_{[800,550]}$ to predict PNA during the jointing stage had better prediction and test results. Our results
257 showed that image parameters can be used to estimate rice N status (especially LAI and AGB). We
258 conclude that image technology can be used as a low-cost, non-destructive, and rapid method to
259 monitor rice N status instead of spectral technology, which could be suitable for the methods used
260 by farmers.

261 **Materials and Methods**

262 **Study Area and Experimental Details**

263 Three independent experiments were performed in this study.

264 Experiment 1 (Exp. 1): This experiment was carried out at the Gao'an base of Jiangxi Academy
265 of Agricultural Sciences (28°25'27" N, 115°12'15" E), Jiangxi Province, China, in 2018. This area
266 is in a mid-subtropical monsoon climate zone, with an annual average temperature of 17.6 °C,
267 annual average sunshine of 1668.2 h, and annual precipitation of 1718.4 mm. The soil properties
268 were as follows: 38.80 g·kg⁻¹ organic matter, 2.53 g·kg⁻¹ total N, 42.4 mg·kg⁻¹ ammonium N, 1.04
269 mg·kg⁻¹ nitrate N, 16.78 mg·kg⁻¹ rapidly available phosphorus (P), 120.1 mg·kg⁻¹ rapidly available
270 potassium (K), and pH 5.5. A split-plot design was used with cultivar as the main plot and N
271 treatment as the sub-plot with three replications. The experiment included two rice cultivars
272 (Conventional rice: Zhonjiaozao17; Hybrid rice: Changliangyou173) and four N application levels
273 (0, 75, 150, 225 kg·hm⁻²). The row and plant spacing was 24 cm × 14 cm. Three seedlings were
274 planted in each hole in the north-south direction. The plots were separated by ridges and were
275 irrigated independently. The plot area was 30 m². Seeds were sown on 23 March and seedlings were

276 transplanted on 23 April at three planting densities. All experimental plots were also supplemented
277 with $75 \text{ kg}\cdot\text{hm}^{-2} \text{ P}_2\text{O}_5$ as P fertilizer and $150 \text{ kg}\cdot\text{hm}^{-2} \text{ K}_2\text{O}$ as K fertilizer. The P fertilizer was added
278 as base fertilizer, and N and K fertilizers were applied at three stages: 40% as base fertilizer, 30%
279 at the tillering stage, and 30% at the ear-filling stage. Other cultivation measures were consistent
280 with local high-yielding cultivation practices.

281 Experiment 2 (Exp. 2): This experiment was carried out at the Gao'an base of Jiangxi Academy
282 of Agricultural Sciences in 2019. The soil properties were as follows: $38.60 \text{ g}\cdot\text{kg}^{-1}$ organic matter,
283 $2.51 \text{ g}\cdot\text{kg}^{-1}$ total N, $42.0 \text{ mg}\cdot\text{kg}^{-1}$ ammonium N, $1.09 \text{ mg}\cdot\text{kg}^{-1}$ nitrate N, $16.88 \text{ mg}\cdot\text{kg}^{-1}$ rapidly
284 available P, $120.3 \text{ mg}\cdot\text{kg}^{-1}$ rapidly available K, and pH 5.5. A split-plot design was used with cultivar
285 as the main plot and N treatment as the sub-plot with three replications. Seeds were sown on 25
286 March and seedlings were transplanted on 24 April at three planting densities. The four N
287 application levels, row spacing, row direction, plot area, and types and amounts of NPK fertilizers
288 were the same as those in Exp. 1.

289 Experiment 3 (Exp. 3): This experiment was carried out at Jiebu, Xingan County ($28^{\circ}25'27''$
290 N, $115^{\circ}12'15''$ E), Jiangxi Province, China in 2019. This area is in a humid subtropical monsoon
291 climate zone, with an annual average temperature of 20.4°C , annual average sunshine of 1684.8 h,
292 and annual precipitation of 1520 mm. The soil properties were as follows: $28.20 \text{ g}\cdot\text{kg}^{-1}$ organic
293 matter, $127.1 \text{ mg}\cdot\text{kg}^{-1}$ available N, $29 \text{ mg}\cdot\text{kg}^{-1}$ rapidly available P, and $120.0 \text{ mg}\cdot\text{kg}^{-1}$ rapidly
294 available K. This experiment included two rice cultivars (Conventional rice: Zaoxian618; Hybrid
295 rice: Xiangzaoxian45) and four N application levels. The four N application levels, row spacing,
296 row direction, plot area, and types and amounts of NPK fertilizers were the same as those in Exp. 1.

297 **Field Data Collection**

298 Repeated destructive sampling was carried out in each plot for Exp. 1 and Exp. 2. Three rice plants
299 from each experimental plot were randomly selected to determine LAI. For each sample, the green
300 leaves were separated from the stems, and the leaf area (LA) was immediately determined by
301 multiplying length by width. The LAI for each plot was calculated based on the planting densities.
302 After bagging, the plant samples were heated in an oven at 105 °C for 30 min, dried to constant
303 weight at 80 °C, and then weighed to determine the dry weight per unit area. Samples were crushed
304 before determining N content using the Kjeldahl method. The PNA value was calculated as follows:

$$305 \text{ PNA (g N·m}^{-2}\text{)} = \text{LNC (\%)} \times \text{LDW (g DW·m}^{-2}\text{)} + \text{SNC (\%)} \times \text{SDW (g DW·m}^{-2}\text{)} + \text{PNC (\%)} \times \text{PDW (g}$$

306 $\text{DW·m}^{-2}\text{)},$

(1)

307 Where LNC is leaf N content, LDW is leaf dry weight, SNC is stem N content, SDW is stem
308 dry weight, PNC is plant N content, and PDW is plant dry weight. Before sampling, images of the
309 rice canopy were obtained using a Canon EOS 100D digital camera (resolution, 72 DPI) (Canon,
310 Tokyo, Japan). The camera lens was about 1.0 m away from the rice canopy at an angle of 60°
311 relative to the ground. The camera was set to auto mode to control the color balance automatically.
312 The images were stored in JPEG format with a resolution of 5184 × 3456 pixels.

313 A FieldSpec Handheld 2 spectroradiometer (Analytical Spectral Devices, Boulder, CO, USA)
314 was used to measure the spectra of the rice plant population. The band range was 325~1075 nm.
315 Spectral data were obtained at the same time as agronomic sampling and image sampling. The
316 vertical height between the probe and the canopy was 1 m. The field of view angle was 25° and
317 reference plate correction was carried out before and after acquiring each target spectrum. The
318 average value was calculated from 10 repeated measurements within the field of view. Five fields

319 of view were analyzed for each plot.

320 **Data Processing and Analysis**

321 1) Image data processing

322 In the periods of rice growth, the canopy does not completely obscure the ground, so images contain
323 soil, water, and other non-canopy items. Consequently, it is necessary to segment and extract the
324 canopy part from the image. Image segmentation eliminates interference from non-canopy items so
325 that data for the crop canopy can be extracted and analyzed. We used the Otsu threshold
326 segmentation algorithm to segment images. This image segmentation method is based on the
327 difference of reflectance spectra between green vegetation and soil in the visible light region.
328 Figures 9a and 9b show the original and segmented images of the rice canopy, respectively (Fig. 9b
329 shows the rice canopy area in white).



330
331
332
333
334
335 (a) (b)

336 **Fig. 9. Canopy images of rice before (a) and after (b) applying Otsu threshold**
337 **segmentation algorithm.**

338 At the same time, the histogram program in Adobe Photoshop 7.0 software was used to obtain
339 the red, green, and blue intensity values of the image. Using combinations of these three color
340 parameters, a variety of color parameters can be obtained. Table 3 showed that the references of

341 image parameters previous researchers used to indirectly characterize crop nitrogen nutrition. In this
 342 study, eight color parameters including image R-G-B were selected.

343 **Table 3 Image characteristic values and calculation methods**

Parameter	Abbreviation	Algorithm formula	Reference
Normalized value of red band	NRI	$NRI=R/R+G+B$	
Normalized value of green band	NGI	$NGI=G/R+G+B$	
Green blue band ratio index	GDR	$GDR=G/R$	
Green blue band difference index	GMR	$GMR=G-R$ if $R=\max$,	
		$H=(G-B)/(\max-\min)*60$	[21]
		if $G=\max$,	
Hue	Hue	$H=120+(B-R)/(\max-\min)*60$ if $B=\max$,	
		$H=240+(R-B)/(\max-\min)*60$	
		if $H<0$, $H=H+360$	

344 2) Spectral data processing

345 Table 4 showed that the references of spectral reflectance parameters previous researchers used to
 346 indirectly characterize crop nitrogen nutrition.

347 **Table 4 Algorithms for different spectral parameters**

Spectral parameter	Abbreviation	Algorithm formula	Reference
Reflectance	R_λ		
Ratio vegetation index	$RVI(\lambda_1, \lambda_2)$	$R_{\lambda 1}/R_{\lambda 2}$	[34]

Differential vegetation index	$DVI(\lambda_1, \lambda_2)$	$R_{\lambda 1} - R_{\lambda 2}$	[34]
Normalized difference vegetation index	$NDVI(\lambda_1, \lambda_2)$	$\frac{ R_{\lambda 1} - R_{\lambda 2} }{R_{\lambda 1} + R_{\lambda 2}}$	[35]
Red edge position wavelength	λ_{rep}	$710 + 50 \times \left(\frac{1/2(R_{870} + R_{660}) - R_{710}}{R_{760} - R_{710}} \right)$	[36]

348 3) Data analysis

349 In the models, the rice N nutrition index was set as the dependent variable, and image
 350 parameters and spectral parameters were set as independent variables. The quantitative relationships
 351 between rice N nutrition indexes and parameters in Exp. 1 and Exp. 2 were fitted and analyzed using
 352 Microsoft Excel 2010 software. We tested various relationships between them (linear function,
 353 exponential function, logarithmic function, polynomial function, and power function), and the
 354 function with the highest R^2 value was selected as the estimation model. Data from Exp. 3 were
 355 used to test the predictive ability of the models. The reliability of each model was evaluated by
 356 calculating the RMSE, relative root mean square error (RRMSE), and R^2 values. A 1:1 relationship
 357 between observed and simulated values was drawn to show the fitting degree and the predictive
 358 effect of the model. The following formulae were used to calculate RMSE and RRMSE:

359
$$RMSE = \sqrt{\frac{1}{n} \times \sum_{i=1}^n (P_i - O_i)^2} , \quad (2)$$

360
$$RRMSE = RMSE / \bar{O_i} \times 100\% . \quad (3)$$

361 In the above formulae, n is the number of samples tested for model test; P_i is the predicted value
 362 of the model, $\bar{P_i}$ is the average value of the predicted value; O_i is the measured value; and $\bar{O_i}$ is
 363 the average value of the measured values.

Declarations

Ethics approval and consent to participate

Not applicable

Consent for publication

Not applicable

Availability of data and materials

Not applicable

Competing interests

The authors declare that they have no competing interests.

Funding

This research was supported by National key R & D projects (2016YFD0300608). Key-Area Research and Development Program of Jiangxi Province [20202BBFL63046, 20202BBFL63044]; National Youth top talent support program; Jiangxi "double thousand program" project funding.

Authors' contributions

YC, LJZ and LYD designed the study; YC and CZS measured rice canopy. YC and CZS managed the field experiment. YC, LY and HH conducted statistical analyses and drafted the manuscript. All authors contributed to the interpretation of results and/or drafting the manuscript. All authors read

and approved the final manuscript.

Acknowledgements

We thank Jennifer Smith, PhD, from Liwen Bianji, Edanz Group China (www.liwenbianji.cn/ac), for editing the English text of a draft of this manuscript.

References

1. Mohammad Y A, J.K., Chim B K, Emily R, Kevin W, Jeremiah M, Guilherme T, Kefyalew G D, William R, *Nitrogen fertilizer management for improved grain quality and yield in winter wheat in Oklahoma*. Journal of Plant Nutrition, 2013. **36**: 749-761.
2. Han, H., et al., *Study on nitrogen removal from rice paddy field drainage by interaction of plant species and hydraulic conditions in eco-ditches*. Environ Sci Pollut Res Int, 2019. **26**(7): 6492-6502.
3. Zhao, X., et al., *Nitrogen runoff dominates water nitrogen pollution from rice-wheat rotation in the Taihu Lake region of China*. Agriculture, Ecosystems & Environment, 2012. **156**: p. 1-11.
4. GAO Shuai, P.Y., SUN Yuming, GUO Junjie, WANG Chengzi, LING NIIng, ZHANG Yan, GUO Shiwei, *Effects of different nitrogen supply on yield and nitrogen utilization of conventional rice and hybrid rice*. Journal of Arid Nanjing Agricultural University, 2018. **6**(41): 1061-1069.
5. E. Raymond Hunt, M.C., Craig S. T. Daughtry, James E. McMurtrey, Charles L. Walthall, *Evaluation of Digital Photography from Model Aircraft for Remote Sensing of Crop Biomass and Nitrogen Status*. 2005.
6. Inoue, Y., Moran, M.S., Horie, T., *Analysis of spectral measurements in paddy field for predicting rice growth and yield based on a simple crop simulation model*. Plant Production Science 1998. **1**: 269–279.
7. Jin J Y, B.Y.L., Yang L P, *Technology and Equipment of Efficient Soil Testing*, in *China Agriculture Press*. 2006: Beijing.
8. Gang Pan, F.-m.L., and Guo-jun Sun, *Digital Camera Based Measurement of Crop Cover for Wheat Yield Prediction*. IEEE, 2007. **47**(2): 135-146.
9. Congress, X.I., *Non-destructive monitoring of rice by hyperspectral in-field spectrometry and UAV-band remote sensing :case study of field-grown rice in north rhine-westphalia,Germany*, in *Remote Sensing and Spatial Information Sciences*, A.B. M. Willkomm, G. Bareth, Editor. 2016: Czech Republic. 12-19.
10. Jiaoyang He, X.Z., Wanting Guo, Yuanyuan Pan, Xia Yao, Tao Cheng, Yan Zhu, Weixing Cao, Yongchao Tian, *Estimation of Vertical Leaf Nitrogen Distribution Within a Rice Canopy Based on Hyperspectral Data*. Frontiers in Plant Science 2020.
11. Jie Li, Y.F., Xiaoke Wang, Jinfeng Peng, Dinghua Yang, Guiling Xu, Qiangxin Luo, Lingli Wang, Da Ou, Wei Su *Stability and applicability of the leaf value model for variable nitrogen application based on SPAD value in rice*. PLOS ONE 2020.
12. A.M. Ali, H.S.T., S. Sharma, Varinderpal-Singh, *Prediction of dry direct-seeded rice yields using chlorophyll meter, leaf color chart and GreenSeeker optical sensor in northwestern India*

Field Crops Research 2014.

13. Lee, K.-J. and B.-W. Lee, *Estimation of rice growth and nitrogen nutrition status using color digital camera image analysis*. European Journal of Agronomy, 2013. **48**: 57-65.
14. Liu, X.-j., et al., *Leaf area index based nitrogen diagnosis in irrigated lowland rice*. Journal of Integrative Agriculture, 2018. **17**(1): 111-121.
15. Liu, K., et al., *Evaluation of grain yield based on digital images of rice canopy*. Plant Methods, 2019. **15**: 28.
16. Wang, Y., et al., *Estimation of Rice Growth Parameters Based on Linear Mixed-Effect Model Using Multispectral Images from Fixed-Wing Unmanned Aerial Vehicles*. Remote Sensing, 2019. **11**(11).
17. Dongyan Zhang, X.Z., Jian Zhang, Yubin Lan, Chao Xu, Dong Liang, *Detection of rice sheath blight using an unmanned aerial system with high-resolution color and multispectral imaging*. PLOS ONE 2018.
18. Jinwen, L., *Determination of Canopy Average SPAD Readings Based on the Analysis of Digital Images*. Agrotechnology, 2014. **03**(01).
19. Jia, B., et al., *Use of a digital camera to monitor the growth and nitrogen status of cotton*. ScientificWorldJournal, 2014. **2014**: 602647.
20. Jia, L., et al., *Use of Digital Camera to Assess Nitrogen Status of Winter Wheat in the Northern China Plain*. Journal of Plant Nutrition, 2004. **27**(3): 441-450.
21. Wang, Y., et al., *Estimating nitrogen status of rice using the image segmentation of G-R thresholding method*. Field Crops Research, 2013. **149**: 33-39.
22. Zhou ZJ, P.F., Thomsen AG, Andersen MN., *A RVI/LAI-reference curve to detect N stress and guide N fertigation using combined information from spectral reflectance and leaf area measurements in potato*. European Journal of Agronomy, 2017. **87**: 1-7.
23. MILLER, J.R., HARE, E. W., WU, J., *<Quantitative characterization of the vegetation red edge reflectance 1 An inverted Gaussian reflectance model.pdf>*. International Journal of Remote Sensing, 1990. **11**: 10.
24. Mistlele, B. and U. Schmidhalter, *Estimating the nitrogen nutrition index using spectral canopy reflectance measurements*. European Journal of Agronomy, 2008. **29**(4): 184-190.
25. Tian Y C, Y.J., Yao X, Cao W X, Zhu Y, *Monitoring canopy leaf nitrogen concentration based on leaf hyperspectral indices in rice[J]. .Acta Agronomica Sinica*, 2010. **36**(9): 1529-1537.
26. Ben Zhao, A.D., Syed Tahir Ata-Ul-Karim, Zhandong Liu, Zhifang Chen, Zhihong Gong, Jiyang Zhang, Junfu Xiao, Zugui Liu, Anzhen Qin, Dongfeng Ning, *Exploring new spectral bands and vegetation indices for estimating nitrogen nutrition index of summer maize*. European Journal of Agronomy 2018. **93**: 113-125.
27. SUN Xiaoxiangm WANG Fangdong, Z.X., XIE Wen, GUO Xi, ***The estimation models of rice leaf nitrogen concentration based on canopy spectrum and BP neural network***. Chinese Journal of Agricultural Resources and Regional Planning, 2019. **40**(35-44).
28. Mulla, D.J., *Twenty five years of remote sensing in precision agriculture: Key advances and remaining knowledge gaps*. Biosystems Engineering, 2013. **114**(4): 358-371.
29. Hadjimitsis, D.G., C.R.I. Clayton, and A. Retalis, *The use of selected pseudo-invariant targets for the application of atmospheric correction in multi-temporal studies using satellite remotely sensed imagery*. International Journal of Applied Earth Observation and Geoinformation, 2009. **11**(3): 192-200.

30. Zhou, X., et al., *Predicting grain yield in rice using multi-temporal vegetation indices from UAV-based multispectral and digital imagery*. ISPRS Journal of Photogrammetry and Remote Sensing, 2017. **130**: 246-255.

31. Shibayama M C, S.T.H., Takada E J, Inoue A H, Morita K H, Yamaguchi T K Y, Takahashi W T R, Kimura A H, *Estimating rice leaf greenness (SPAD) using fixed-point continuous observations of visible red and near infrared narrow-band digital images*. Plant Production Science, 2012. **15**(4): 293-309.

32. J, P.S.C.K.G.K.M., *Relationship between leaf photosynthesis and nitrogen content of field-grown rice in tropics*. Crop Science, 1995. **6**(35): 1627-1630.

33. S. G. Bajwa, A.R.M., R. J. Norman, *Canopy reflectance response to plant nitrogen accumulation in rice*. Precision Agriculture, 2010. **11**: 488-506.

34. Jordan, C.F., *Derivation of Leaf-Area Index from Quality of Light on the Forest Floor*. Ecology, 1969. **50**.

35. Rouse, J.W.H., R.H.; Schell, J.A.; Deering, D.W. . *Monitoring vegetation systems in the great plains with ERTS*. in *In Third Earth Resources Technology Satellite-1 Symposium-Volume I: Technical Presentation*. 1974. Washington, DC, USA, : NASA.

36. Liu, M., et al., *Monitoring stress levels on rice with heavy metal pollution from hyperspectral reflectance data using wavelet-fractal analysis*. International Journal of Applied Earth Observation and Geoinformation, 2011. **13**(2): 246-255.